Self-Organization of Amine-Based Cathode Interfacial Materials in Inverted Polymer Solar Cells

Di Ma,[†,‡,#] Menglan Lv,[†,§,∥,#] Ming Lei,[⊥,*] Jin Zhu,[§] Haiqiao Wang,[‡,*] and Xiwen Chen[†,*]

[†]CSIRO Materials Science and Engineering, Clayton, VIC 3168, Australia, [‡]State Key Laboratory of Organic—Inorganic Composites, Key Laboratory of Carbon Fiber and Functional Polymers, Ministry of Education, Beijing University of Chemical Technology, Beijing 100029, China, [§]Chengdu Institute of Organic Chemistry, Chinese Academy of Sciences, Chengdu 610041, China, [⊥]Department of Chemistry, Zhejiang University, Hangzhou 310027 China, and [∥]University of Chinese Academy of Sciences, Beijing 100049, China. [#]These authors contributed equally.

ABSTRACT We present a strategy to fabricate polymer solar cells in inverted geometry by self-organization of alcohol soluble cathode interfacial materials in donor—acceptor bulk heterojunction blends. An amine-based fullerene [6,6]-phenyl-C61-butyric acid 2-((2-(dimethylamino)-ethyl)(methyl)amino)ethyl ester (PCBDAN) is used as an additive in poly(3-hexylthiophene) (P3HT) and 6,6-phenyl C_{61}-butyric acid methyl ester (PCBM) blend to give a power conversion efficiency of 3.7% based on devices ITO/P3HT:PCBM:PCBDAN/MoO_3/Ag where the ITO alone is used as the cathode. A vertical phase separation in favor of the inverted device architecture is formed: PCBDAN is rich on buried ITO surface reducing its work function, while P3HT is rich on air interface with the hole-collecting electrode. The driving force of the vertical phase separation is ascribed to the surface energy and its components of the blend compositions and the substrates. Similar results are also found with another typical alcohol soluble cathode interfacial materials, poly[(9,9-bis(3′-(*N*, *N*-dimethylamino)propyl)-2,7-fluorene)-*alt*-2,7-(9,9-dioctylfluorene)] (PFN), implying that self-organization may be a general phenomenon in ternary blends. This self-organization procedure could eliminate the fabrication of printing thin film of interlayers or printing on such thin interlayers and would have potential application for roll-to-roll processing of polymer solar cells.

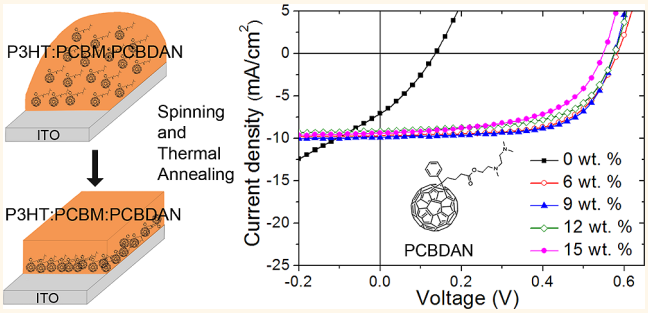

KEYWORDS: self-assembly · conjugated polymers · photovoltaic devices · organic electronics · fullerenes

Polymer solar cells (PSCs) have attracted attention with a promising future of being lightweight, flexible, and attainable *via* roll-to-roll manufacturing process with low cost.[1] Significant progress has been made on donor and acceptor materials, morphological control and bulk heterojunction device architectures.[2−5] One important advance is on the interfacial layers, which have shown various functions for improvement of device performance, such as building selective contacts with tunable work functions for respective charge carriers, working as optical spacers and physical barriers from metal diffusion.[3,6,7]

The cathode interfacial materials have gained significant progress recently as they can avoid use of low work function active metal electrodes.[8−38] Cao *et al.* reported alcohol soluble conjugated polymers with amine or ammonium salts as cathode interfacial layers initially in organic light emitting diodes,[8−11] then in PSCs with significant enhancement of the performance.[12−20] Other alcohol soluble conjugated polymers including hyperbranched polymers and polyfluorenes grafted with K^+ intercalated crown ethers also worked very well.[21−23] In addition, due to the electron transport properties of fullerene derivatives, they have been studied widely as well.[24−33] Jen and his co-workers presented a series of fullerene-based self-assembled monolayers and some alcohol soluble self-n-doped conducting fullerenes.[25−28] Recently, fullerenes with amino-groups or ammonium salts or phosphate were also reported as cathode interfacial materials.[29−33]

In addition to the spin-casted interlayers, self-organization is another way to form cathode interlayers. Fullerene derivatives with a fluorocarbon or a polyethylene oxide

* Address correspondence to xwchen5702@hotmail.com, leiming@zju.edu.cn, Wanghaiqiao@mail.buct.edu.cn.

Received for review November 14, 2013 and accepted January 9, 2014.

Published online January 09, 2014
10.1021/nn4059067

chain were reported to form monolayers on top of photoactive layers.[35−38] Yang *et al.* also found similar phenomenon with poly(vinylpyrrolidone) and oleamide recently.[39,40] This vertical phase separation was originally found in donor/acceptor blends before,[41,42] and it also correlated the fullerene surface coverage and contact selectivity recently.[43] The variation of solvent-evaporation rate has been proved to affect the morphology of films and the formation of donor−acceptor domains. When specifically choosing and altering the surface energies of the ingredients and the substrates, desired phase segregation in favor of inverted device structures could be obtained.[42] The inverted device structure has been used for achieving record single heterojunction PSCs with a PCE of 9.35% and tandem PSC with 10.6%,[44,45] respectively. For inverted structures, organic cathode interlayers were usually deposited before photoactive layer and they needed to be solvent-resistant and the thickness to be very thin.[18,20] Printing such thin films or printing other layers on this kind of thin films has proven challenging.[46,47] Thus, incorporation of cathode interfacial materials by their self-organization in photoactive layers for inverted devices would be very attractive for printable PSCs.

In present work, we demonstrate that vertical phase separation in favor of inverted PSCs with ITO as the cathode is also realized in a ternary blend: a small amount of PCBDAN in P3HT and 6,6-phenyl C_{61}-butyric acid methyl ester (PCBM) blend can self-organize and PCBDAN is rich at the buried ITO surface, whereas P3HT is rich at the air interface with the anode MoO_3/Ag. A moderate PCE of 3.7% is obtained by this simple method and this concept is also proved with another interlayer poly[(9,9-bis(3′-(*N*,*N*-dimethylamino)propyl)-2,7-fluorene)-*alt*-2,7-(9,9-dioctylfluorene)] (PFN).

RESULTS AND DISCUSSION

We noted that a recent paper claimed that amino-based materials function as hole traps, and thus, all the conventional PSCs containing the amine materials did not work.[31] We also found that conventional PSCs with ITO/PEDOT-PSS as the anode did not work in the presence of small amount of PCBDAN in several donor/acceptor blends. Considering the fact that good organic light-emitting diodes (OLEDs) have been reported from electroluminescent conjugated polymers with amino groups,[11] hole traps could not explain the high efficiency in OLEDs and thus the real physics behind could be different. Our hypothesis was that the PCBDAN may migrate to the PEDOT-PSS surface and reduce its work function, resulting in a high hole collection barrier for the devices, and made the conventional cells failed.

As materials with amine group generally reduce the work functions of metals, metal oxides and conducting polymers,[34] Scanning Kelvin Probe Microscopy (SKPM) was used to check how PCBDAN works on various substrates. SKPM provides the contact potential difference (CPD) between the probe tip and the surface, which for a conductive film is related to a relative difference of the work functions. The work functions of PCBDAN on top of various substrates including bare ITO substrate, PEDOT-PSS film on ITO, and evaporated MoO_3 on ITO were measured, and the results are summarized in Table 1. Each value was calculated relative to that of ITO, which was set at a nominal value of 4.70 eV.[23] The work functions of PCBDAN on all the studied substrates were reduced with the increase of PCBDAN solution concentration. When the concentration increased to 6 mg/mL (corresponding to a thickness of 13 nm), the work function no longer changed and kept at ∼4.1 eV for PCBDAN on all the substrates. The work function for $PC_{71}BM$ is 5.1 eV,[43] so the reduction of work function is attributed to the amine functional group. These results confirmed that interfacial dipole does exist on various substrates including conducting metal oxide, semiconducting metal oxide and conducting polymer. The fact of reduction of work functions of ITO and PEDOT-PSS is encouraging, but the reduction of work function of MoO_3 is surprising since MoO_3 has been used successfully as hole collection layer on top of amino-based cathode interfacial layers.[12,23] Thus, the MoO_3 layer was put upside down: the evaporated MoO_3 layer was on top of various substrates and its work function was measured with SKPM as well (Table 2). For the MoO_3 film thickness over 5 nm that has been tested, MoO_3 has high work function over 5.3 eV, implying that 5 nm thick MoO_3 could be used as efficient hole collection layer.

Thus, inverted devices ITO/P3HT:PCBM:PCBDAN/MoO_3/Ag with PCBDAN as an additive and ITO alone as the cathode were fabricated and tested as shown in Scheme 1. The device performance data extracted

TABLE 1. Work Functions (in eV) of PCBDAN on Various Substrates Measured by Scanning Kelvin Probe Microscopy in Air[a]

film[b]	12	6	3	1	0.5	0.05	0
A	4.11	4.14	4.19	4.28	4.45	4.67	4.70
B	4.12	4.12	4.13	4.24	4.39	4.43	5.10
C	4.09	4.09	4.09	4.19	4.38	5.08	5.56

[a] The work function of ITO was set as 4.70 eV. The errors of measured work function are ±0.025 eV. [b] A, ITO/; B, ITO/PEDOT:PSS(38 nm)/; C, ITO/MoO_3(40 nm)/. PCBDAN cast from indicated concentration (mg/mL).

TABLE 2. Work Functions (in eV) of Evaporated MoO_3 on Various Substrates Measured by Scanning Kelvin Probe Microscopy in Air

thickness of MoO_3 (nm)	none	5	10	15
ITO /	4.70	5.39	5.46	5.56
ITO/PCBDAN (90 nm)/	4.07	5.33	5.44	5.54

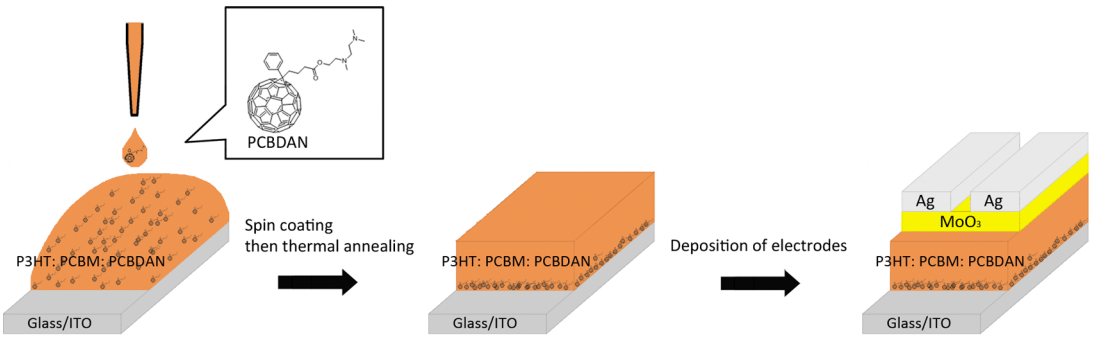

Scheme 1. Procedure of fabricating devices with PCBDAN as the additive in P3HT:PCBM blend and molecular structure of PCBDAN.

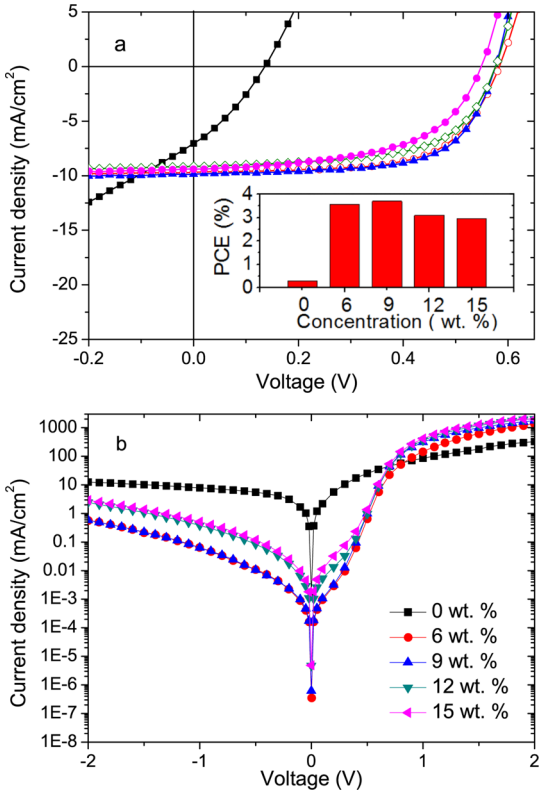

Figure 1. Current density–voltage (*J*–*V*) characteristics of the devices with PCBDAN (amount indicated) blended in P3HT and PCBM blend (a) under 1000 W/m^2 at AM 1.5G illumination and (b) dark.

TABLE 3. Performance of Devices ITO/P3HT:PCBM: PCBDAN/MoO_3/Ag with Different Amount of PCBDAN (Relative to PCBM)

PCBDAN [wt %]	V_{oc} [V]	J_{sc} [mA cm^{-2}]	FF [%]	PCE (average) [%]	R_{sh} [kΩ cm^2]	R_s [Ω cm^2]
0	0.14	7.05	30.3	0.30 (0.28)	0.03	5.84
6.0	0.58	9.55	64.5	3.57 (3.45)	38.27	0.89
9.0	0.58	9.87	64.6	3.70 (3.66)	38.27	0.89
12.0	0.56	9.41	58.7	3.09 (3.02)	15.57	0.86
15.0	0.55	9.54	56.6	2.97 (2.92)	3.77	0.78

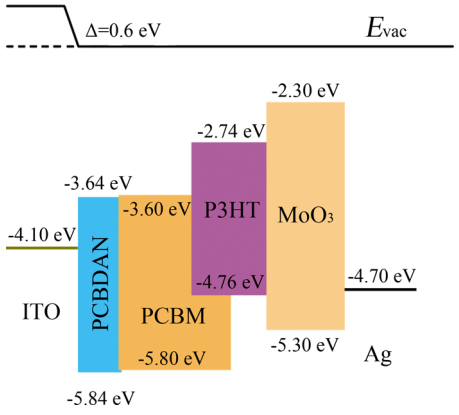

Figure 2. Energy band diagram of devices with PCBDAN as the additive.

from the current density *versus* voltage (*J*–*V*) characteristics in Figure 1 is shown in Table 3. The blank devices without PCBDAN in the blend performed poor with a PCE of only 0.30% and had low open circuit voltage (V_{oc}), short circuit current (J_{sc}) and fill factor (FF). This was expected as the ITO alone is not suitable as the cathode. In the presence of small amount of PCBDAN, the inverted devices can work normally. At an optimized amount of PCBDAN of 9.0 wt % (relative to PCBM) as seen from inset of Figure 1a, the PCE reached 3.7% with a V_{oc} of 0.58 V, a J_{sc} of 9.87 mA cm^{-2}, and a FF of 64.6%. This performance is comparable to typical inverted devices reported in literature in the presence of cathode interlayers.[15–17] The energy band diagram of the devices with the additive is shown in Figure 2, as will be discussed below.

The well-performed inverted devices may suggest that small amount of PCBDAN migrated to the buried ITO surface and reduced the work function of ITO for its use as the cathode directly. To confirm the formation of the favorable vertical phase separation structure for the inverted devices, X-ray photoelectron spectroscopy (XPS) was used to detect the compositions on air interface with the active layer. The depth profile was not performed as the atomic ratio of N/C in the blend is below the detection limit of the instrument. The results are shown in Table 4. No nitrogen was detected,

indicating PCBDAN was not detectable at air interface of the ternary blend. The surface S/C ratio was 0.063, much higher than that (0.041) calculated for the ternary blend. These collective results imply that P3HT is rich at the air interface. Although PCBDAN was not detectable with XPS, its coverage on the buried ITO interface could be evidenced from the device performance. Up to a concentration of about 9 wt %, the coverage of PCBDAN at the ITO surface could be optimized. At higher content, the PCBDAN could go into the active layer forming a ternary blend which could have reduced performance. To study the surface properties of the materials and substrates, advancing contact angle measurement was conducted. The method called "Three-Liquid Acid-Base Method" was developed by van Oss, Good, and their co-workers which theoretically based on the two-liquid geometric method and two-liquid harmonic method.[48−50] As described in the Supporting information, films were obtained by spin-casting solutions onto the ITO substrates. Water, ethylene glycol and hexadecane were chosen as the three probing liquids. Values of measured contact angles and calculated surface energies and their components are summarized in Table 5. The surface energies of PCBDAN (30.4 mN m^{-1}) and PCBM (28.1 mN m^{-1}) films were relatively similar with each other, whereas that of P3HT film (23.8 mN m^{-1}) was lower. The two blend films (P3HT:PCBM and P3HT:PCBM:PCBDAN) had similar surface energy at 24.1 mN m^{-1} which was almost the same as that of P3HT film. Other surface energy components were also very similar for these three films containing P3HT, indicating that the air interface with the blend films was capped with a very thin layer of P3HT. Similar phenomenon has been reported in other blends before.[51] The XPS results showed only P3HT rich at air interface, which could be explained by detectable PCBDAN underneath this thin layer. In addition, the electron donor components of the surface energy, γ^-, for ITO and PCBDAN are 75.0 and 68.1 mN m^{-1}, which were significantly higher than those of the other films. The similar Lewis base interaction and close surface energies for ITO and PCBDAN could drive PCBDAN toward the buried ITO interface, similar to P3HT:PCBDAN binary blend

TABLE 4. Surface Atomic Ratios of Elements Obtained by XPS Analysis

	measured atomic ratio (X/C)				calculated atomic ratio (X/C)[a]			
film	C/C	N/C	O/C	S/C	C/C	N/C	O/C	S/C
ITO/PCBDAN	1.00	0.026	0.026	0	1.00	0.026	0.026	0
ITO/P3HT	1.00	0	0.003	0.081	1.00	0	0	0.100
ITO/P3HT: PCBM: PCBDAN	1.00	0	0.013	0.063	1.00	0.001	0.016	0.041

[a] Calculated from solids in solutions for spin-cast films.

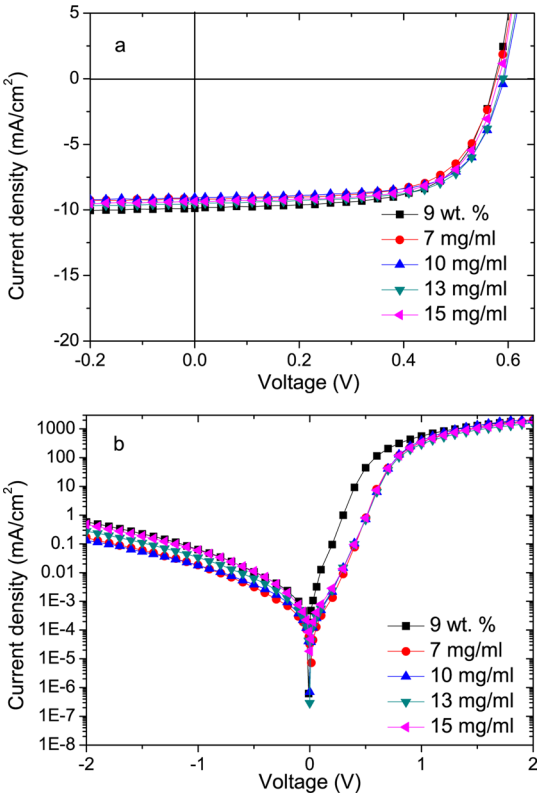

Figure 3. Current density−voltage ($J-V$) characteristics of the devices ITO/PCBDAN/P3HT:PCBM/MoO_3/Ag with PCBDAN interlayer (solution concentration indicated) (a) under 1000 W/m^2 at AM 1.5G illumination and (b) dark. PCBDAN as additive (9 wt %) included for comparison.

TABLE 5. Advancing Contact Angles of Three Probing Liquids on Various Surfaces at Initial State, And the Calculated Surface Energies (mN m^{-1})

		ITO	PCBDAN	PCBM	P3HT	P3HT:PCBM	P3HT:PCBM:PCBDAN
Contact angle (deg)	Water	14 ± 1	33 ± 3	82 ± 1	107 ± 1	108 ± 1	107 ± 1
	Ethylene Glycol	27 ± 2	45 ± 3	61 ± 1	79 ± 1	78 ± 1	80 ± 1
	Hexadecane	15 ± 1	15 ± 1	13 ± 1	31 ± 1	30 ± 1	29 ± 1
Calculated surface energy component (mN m^{-1})	γ	40.0	30.4	28.1	23.9	24.1	24.1
	γ^{LW}	26.4	26.4	26.6	23.8	24.0	24.0
	γ^{AB}	14	4.0	1.5	0.14	0.06	0.13
	γ^+	0.62	0.06	0.25	0.08	0.11	0.05
	γ^-	75.0	68.1	8.5	0.07	0.01	0.08

TABLE 6. Performance Data of Devices with a PCBDAN Interlayer

PCBDAN interlayer [mg mL^{-1}]	*Voc* [V]	*Jsc* [mA cm^{-2}]	FF [%]	PCE (average) [%]	*Rsh* [kΩ cm^2]	R_s [Ω cm^2]
7	0.58	9.20	65.8	3.51 (3.50)	117.10	0.65
10	0.58	9.90	67.0	3.85 (3.83)	73.64	0.55
13	0.59	9.51	66.8	3.75 (3.75)	56.82	0.82
15	0.58	9.62	66.0	3.69 (3.68)	58.51	0.72

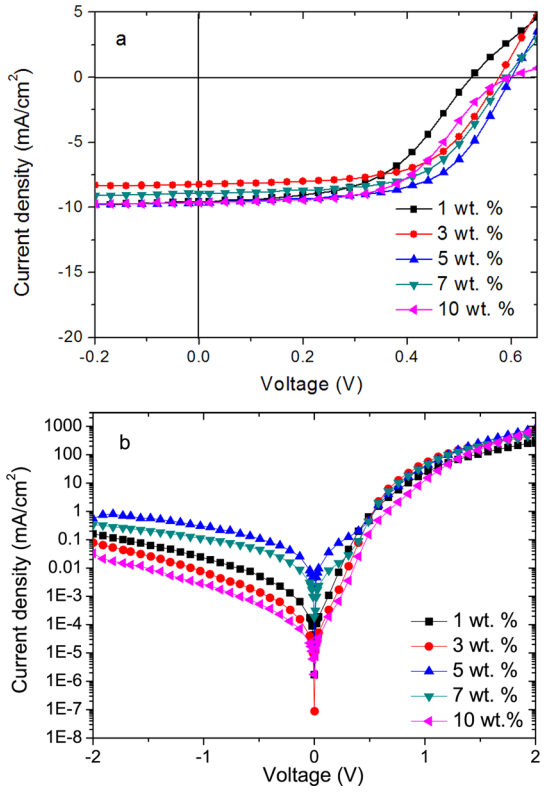

Figure 4. Current density–voltage (*J*–*V*) characteristics of the devices with PFN (amount indicated) blended in P3HT and PCBM blend (a) under 1000 W/m^2 at AM 1.5G illumination and (b) dark.

as we observed (unpublished work). It was reported that the buried interface of P3HT:PCBM blend on PEDOT-PSS is characterized by thermodynamically stable composition profiles.[51] In combination with the device performance, the thermodynamic analysis for the buried interface between the ternary blend and ITO could also be most probably applicable. In addition, PEDOT-PSS was reported to have similar surface energy and its components to ITO.[51] Thus PCBDAN could also be rich at the buried interface between PEDOT-PSS and photoactive layers, which resulted in failure in our conventional devices with PEDOT-PSS as the hole-collecting layer as well as in literature.[31]

To gain evidence of the self-organization in another way, bilayer devices ITO/PCBDAN/P3HT:PCBM/MoO_3/Ag were fabricated, where PCBDAN film was spin-cast as a cathode interlayer (see Figure 3 and Table 6 for device performance). At an optimized concentration of 10 mg mL^{-1} PCBDAN for the spin-cast interlayer, a PCE of 3.85% was obtained with V_{oc} of 0.58 V, J_{sc} of 9.90 mA cm^{-2}, and FF of 67.0%. This performance is comparable to that with PCBDAN as the additive, suggesting a similar vertical phase separation to some extent, and thus the bilayer process could be simplified by additive self-organization.

TABLE 7. Performance Data of Devices with PFN as the Additive

PFN [wt %]	V_{oc} [V]	J_{sc} [mA cm^{-2}]	FF [%]	PCE (average) [%]	R_{sh} [kΩ cm^2]	R_s [Ω cm^2]
1.0	0.52	9.55	53.4	2.65 (2.62)	32.39	6.08
3.0	0.58	8.31	62.3	3.00 (2.89)	45.48	3.05
5.0	0.60	9.61	60.6	3.50 (3.49)	36.08	2.63
7.0	0.59	8.94	59.7	3.15 (3.12)	15.13	3.21
10.0	0.60	9.65	53.9	3.12 (3.09)	61.20	3.94

To check if the self-organization of the amine-based cathode interfacial materials in present donor/acceptor ternary blend is a general phenomenon, the PFN, a typical alcohol soluble conjugated polymer soluble in dichlorobenzene as well, was also used as an additive in inverted PSCs in the same way. The device performance data extracted from Figure 4 is shown in Table 7. At an optimized concentration of 5.0 wt % PFN (relative to PCBM), a PCE of 3.5% was obtained with V_{oc} of 0.60 V, J_{sc} of 9.61 mA cm^{-2}, and FF of 60.6%. Thus, self-organization of amino-based cathode interfacial materials in photoactive blends could be a general phenomenon. We note that the PCE and optimized amount of PCBDAN as the additive are slightly higher than that of PFN. The conductivity, the diffusion and solubility of the additives may vary and make some difference on the device performance.

CONCLUSION

We have demonstrated that amino-based cathode interfacial materials such as PCBDAN and PFN could be added in P3HT:PCBM blend for making inverted PSCs with ITO as the cathode. Vertical phase separation driven by the various surface energies of blend components and the substrate is in favor of the inverted device architecture. PCBDAN is rich at the buried interface with ITO and, therefore, reduces the work function of ITO for its use as the cathode, while very thin layer of

P3HT is at the air interface with MoO_3/Ag for hole collection. Through this strategy, a PCE of 3.70% was obtained in the inverted devices. Our facile strategy incorporating the cathode interlayer materials in the photoactive blends may have potential applications in organic electronics for roll-to-roll processing and on flexible substrates, as there is no need to fabricate a thin layer of organic cathode interfacial materials, neither a layer of ZnO or TiO_x *etc.* which usually need thermal annealing process.

METHODS

Materials. All solvents were purchased from Sigma Aldrich, P3HT from Merck Chemicals Ltd. and PCBM from Nano-C, Inc. PCBDAN was synthesized with literature method.[30] PFN was synthesized in accordance with literature method.[10]

Device Fabrication. The ITO-coated glass substrates were first cleaned *via* a four-step solvent cleaning procedure under sonicating which started from detergent, then deionized water, acetone and isopropyl alcohol, each for 10 min. Then the substrates were dried before undertaking a 10 min ultraviolet-ozone treatment. After that, the substrates were transferred into a glovebox with nitrogen atmosphere. A ternary blend of P3HT, PCBM and PCBDAN was dissolved in dichlorobenzene and heated in 90 °C for 1 h. The concentration of P3HT was 15 mg mL^{-1} and P3HT and PCBM were in weight ratio of 1:1. For device optimization, PCBDAN was added in different weight ratios relative to PCBM. The solution of the active layer was spin coated onto the ITO coated substrates at a spin speed of 1300 rpm for 1 min and then thermally annealed at 150 °C for 10 min to give a thickness around 100 nm, measured with Dektak 6 M Stylus Profiler (Veeco, Inc.). A molybdenum trioxide layer with 10 nm thick was deposited on the active layer at rate of 0.2 Å/s and then a silver layer with a thickness of 100 nm at rate of 3 Å/s at a pressure below 2×10^{-6} Torr. The defined device with masks was 0.10 cm^2. In case of PFN as the additive, PCBDAN was replaced by PFN in the above process and the weight percent of PFN is relative to that of PCBM.

The devices using PCBDAN as a cathode interlayer were also prepared in nitrogen atmosphere. The solutions of PCBDAN in chlorobenzene at different concentrations were spin-cast on ITO substrates. The PCBDAN was dissolved in chlorobenzene in 90 °C for 1 h and a spin rate of 1000 rpm for 30 s was utilized for spin-casting films. An active layer of P3HT and PCBM was spin coated onto the PCBDAN film in the same condition as the devices with the additive. The devices were made by the same thermal annealing process and had the same hole collection layer and anode (MoO_3/Ag). The procedure of preparing blank devices was the same except no PCBDAN was used. The devices with PFN as the additive were made similarly.

Film and Device Characterization. Current density−Voltage (*J*−*V*) characteristics of the devices were measured with an Oriel solar simulator fitted with a 1000 W Xe lamp filtered to give an output of 100 mW/cm^2 at AM 1.5G. The Xenon lamp was calibrated using a standard filtered Silicon reference cell (Peccell Limited, Inc.). The devices were tested using a Keithley 2400 Source meter controlled by Labview software. The contact angles were measured with a CAM 200 (KSV Instrument LID). The surface potentials were measured on an SKP5050 K probe system (KP Technology) in air. The work functions were achieved from an average value of 200 points for each sample.

X-ray photoelectron spectroscopy (XPS) analysis was performed using an AXIS Ultra DLD spectrometer (Kratos Analytical, Inc., Manchester, U.K.) with a monochromated Al K_γ source at a power of 150 W (15 kV × 10 mA), a hemispherical analyzer operating in the fixed analyzer transmission mode and the standard aperture (analysis area: 0.3 mm × 0.7 mm). The total pressure in the main vacuum chamber during analysis was typically between 10^{-9} and 10^{-8} mbar.

Conflict of Interest: The authors declare no competing financial interest.

Acknowledgment. This work was supported by CSIRO through CSIRO-CAS (Chinese Academy of Sciences) joint project and the Victorian Organic Solar Cell Consortium (Victorian Department of Primary Industries, Sustainable Energy Research and Development Grant and Victorian Department of Business and the Australian Solar Institute). We thank Dr. Chris D. Easton for XPS measurements.

Supporting Information Available: Calculation of surface energy of various films. This material is available free of charge *via* the Internet at http://pubs.acs.org.

REFERENCES AND NOTES

1. Yang, J.; You, J.; Chen, C. C.; Hsu, W. C.; Tan, H. R.; Zhang, X. W.; Hong, Z.; Yang, Y. Plasmonic Polymer Tandem Solar Cell. *ACS Nano* **2011**, *5*, 6210–6217.
2. Brabec, C. J.; Gowrisanker, S.; Halls, J. J. M.; Laird, D.; Jia, S.; Williams, S. P. Polymer−Fullerene Bulk-Heterojunction Solar Cells. *Adv. Mater.* **2010**, *22*, 3839–3856.
3. Li, C. Z.; Yip, H. L.; Jen, A. K.-Y. Functional Fullerenes for Organic Photovoltaics. *J. Mater. Chem.* **2012**, *22*, 4161–4177.
4. He, Y. J.; Li, Y. F. Fullerene Derivative Acceptors for High Performance Polymer Solar Cells. *Phys. Chem. Chem. Phys.* **2011**, *13*, 1970–1983.
5. Steim, R.; Koglera, F. R.; Brabec, C. J. Interface Materials for Organic Solar Cells. *J. Mater. Chem.* **2010**, *20*, 2499–2512.
6. Hayakawa, A.; Yoshikawa, O.; Fujieda, T.; Uehara, K.; Yoshikawa, S. High Performance Polythiophene/Fullerene Bulk-Heterojunction Solar Cell with a TiOx Hole Blocking Layer. *Appl. Phys. Lett.* **2007**, *90*, 163517.
7. Lee, K.; Kim, J. Y.; Park, S. H.; Kim, S. H.; Cho, S.; Heeger, A. J. Air-Stable Polymer Electronic Devices. *Adv. Mater.* **2007**, *19*, 2445–2449.
8. Duan, C. H.; Zhang, K.; Zhong, C. M.; Huang, F.; Cao, Y. Recent Advances in Water/Alcohol-Soluble p-Conjugated Materials: New Materials and Growing Applications in Solar Cells. *Chem. Soc. Rev.* **2013**, *42*, 9071–9104.
9. Huang, F.; Wu, H. B.; Cao, Y. Water/Alcohol Soluble Conjugated Polymers as Highly Efficient Electron Transporting/Injection Layer in Optoelectronic Devices. *Chem. Soc. Rev.* **2010**, *39*, 2500–2521.
10. Huang, F.; Wu, H. B.; Wang, D. L.; Yang, W.; Cao, Y. Novel Electroluminescent Conjugated Polyelectrolytes Based on Polyfluorene. *Chem. Mater.* **2004**, *16*, 708–716.
11. Huang, F.; Hou, L. T.; Wu, H. B.; Wang, X. H.; Shen, H. L.; Cao, W.; Yang, W.; Cao, Y. High-Efficiency, Environment-Friendly Electroluminescent Polymers with Stable High Work Function Metal as a Cathode: Green- and Yellow-Emitting Conjugated Polyfluorene Polyelectrolytes and Their Neutral Precursors. *J. Am. Chem. Soc.* **2004**, *126*, 9845–9853.
12. He, Z. C.; Zhong, C. M.; Huang, X.; Wong, W. Y.; Wu, H. B.; Chen, L. W.; Su, S. J.; Cao, Y. Simultaneous Enhancement of Open-Circuit Voltage, Short-Circuit Current Density, and Fill Factor in Polymer Solar Cells. *Adv. Mater.* **2011**, *23*, 4636–4643.
13. Yang, T. B.; Wang, M.; Duan, C. H.; Hu, X. W.; Huang, L.; Peng, J. B.; Huang, F.; Gong, X. Inverted Polymer Solar Cells with 8.4% Efficiency by Conjugated Polyelectrolyte. *Energy Environ. Sci.* **2012**, *5*, 8208–8214.
14. Chang, Y. M.; Zhu, R.; Richard, E.; Chen, C. C.; Li, G.; Yang, Y. Electrostatic Self-Assembly Conjugated Polyelectrolyte-Surfactant Complex as an Interlayer for High Performance Polymer Solar Cells. *Adv. Funct. Mater.* **2012**, *22*, 3284–3289.

15. Worfolk, B. J.; Hauger, T. C.; Harris, K. D.; Rider, D. A.; Fordyce, J. A. M.; Beaupré, S.; Leclerc, M.; Buriak, J. M. Work Function Control of Interfacial Buffer Layers for Efficient and Air-Stable Inverted Low-Bandgap Organic Photovoltaics. *Adv. Energy Mater.* **2012**, *2*, 361–368.
16. Sun, K.; Zhao, B.; Kumar, A.; Zeng, K.; Ouyang, J. Highly Efficient, Inverted Polymer Solar Cells with Indium Tin Oxide Modified with Solution-Processed Zwitterions as the Transparent Cathode. *ACS Appl. Mater. Interfaces* **2012**, *4*, 2009–2017.
17. Murugesan, V.; Sun, K.; Ouyang, J. Y. Highly Efficient Inverted Polymer Solar Cells With a Solution-Processable Dendrimer as the Electron-Collection Interlayer. *Appl. Phys. Lett.* **2013**, *102*, 83302.
18. Liu, S. J.; Zhang, K.; Lu, J. M.; Zhang, J.; Yip, H. L.; Huang, F.; Cao, Y. High-Efficiency Polymer Solar Cells *via* the Incorporation of an Amino-Functionalized Conjugated Metallopolymer as a Cathode Interlayer. *J. Am. Chem. Soc.* **2013**, *135*, 15326–15329.
19. Duan, C. H.; Zhang, K.; Guan, X.; Zhong, C. M.; Xie, H. M.; Huang, F.; Chen, J. W.; Peng, J. B.; Cao, Y. Conjugated Zwitterionic Polyelectrolyte-Based Interface Modification Materials for High Performance Polymer Optoelectronic Devices. *Chem. Sci.* **2013**, *4*, 1298–3107.
20. Dong, Y.; Hu, X. W.; Duan, C. H.; Liu, P.; Liu, S. J.; Lan, L. Y.; Chen, D. C.; Yang, L.; Su, S. J.; Gong, X.; *et al.* A Series of New Medium-Bandgap Conjugated Polymers Based on Naphtho[1,2-c:5,6-c]bis(2-octyl-[1,2,3]triazole) for High-Performance Polymer Solar Cells. *Adv. Mater.* **2013**, *25*, 3683–3688.
21. He, Z. C.; Zhong, C. M.; Su, S. J.; Xu, M.; Wu, H. B.; Cao, Y. Enhanced Power-Conversion Efficiency in Polymer Solar Cells Using an Inverted Device Structure. *Nat. Photonics* **2012**, *6*, 591–595.
22. Liao, S. H.; Li, Y. L.; Jen, T. H.; Cheng, Y. S.; Chen, S. A. Multiple Functionalities of Polyfluorene Grafted with Metal Ion-Intercalated Crown Ether as an Electron Transport Layer for Bulk-Heterojunction Polymer Solar Cells: Optical Interference, Hole Blocking, Interfacial Dipole, and Electron Conduction. *J. Am. Chem. Soc.* **2012**, *134*, 14271–14274.
23. Lv, M. L.; Li, S. S.; Jasieniak, J. J.; Hou, J. H.; Zhu, J.; Tan, Z. H.; Watkins, S. E.; Li, Y. F.; Chen, X. W. A Hyperbranched Conjugated Polymer as the Cathode Interlayer for High Performance Polymer Solar Cells. *Adv. Mater.* **2013**, *25*, 6889–6894.
24. Qu, S. X.; Li, M. H.; Xie, L. X.; Huang, X.; Yang, J. G.; Wang, N.; Yang, S. F. Noncovalent Functionalization of Graphene Attaching [6,6]-Phenyl-C61-butyric Acid Methyl Ester (PCBM) and Application as Electron Extraction Layer of Polymer Solar Cells. *ACS Nano* **2013**, *7*, 4070–4081.
25. Li, C. Z.; Chueh, C. C.; Yip, H. L.; O'Malley, K. M.; Chen, W. C.; Jen, A. K.-Y. Effective Interfacial Layer to Enhance Efficiency of Polymer Solar Cells *via* Solution-Processed Fullerene-Surfactants. *J. Mater. Chem.* **2012**, *22*, 8574–8578.
26. Hau, S. K.; Cheng, Y. J.; Yip, H. L.; Zhang, Y.; Ma, H.; Jen, A. K.-Y. Effect of Chemical Modification of Fullerene-Based Self-Assembled Monolayers on the Performance of Inverted Polymer Solar Cells. *ACS Appl. Mater. Interfaces* **2010**, *2*, 1892–1902.
27. O'Malley, K. M.; Li, C. Z.; Yip, H. L.; Jen, A. K.-Y. Enhanced Open-Circuit Voltage in High Performance Polymer/Fullerene Bulk-Heterojunction Solar Cells by Cathode Modification with a C60 Surfactant. *Adv. Energy Mater.* **2012**, *2*, 82–86.
28. Li, C. Z.; Chueh, C. C.; Yip, H. L.; Ding, F.; Li, X.; Jen, A. K.-Y. Solution-Processible Highly Conducting Fullerenes. *Adv. Mater.* **2013**, *25*, 2457–2461.
29. Hong, D.; Lv, M. L.; Lei, M.; Chen, Y.; Lu, P.; Wang, Y. G.; Zhu, J.; Wang, H. Q.; Gao, M.; Watkins, S. E.; *et al.* N-Acyldithieno-[3,2-b:2′,3′-d]pyrrole-based Low Bandgap Conjugated Polymer Solar Cells with Amine-Modified [6,6]-Phenyl-C61-butyric Acid Ester Cathode Interlayers. *ACS Appl. Mater. Interfaces* **2013**, *5*, 10995–11003.
30. Li, S. S.; Lei, M.; Lv, M. L.; Watkins, S. E.; Tan, Z. A.; Zhu, J.; Hou, J. H.; Chen, X. W.; Li, Y. F. [6,6]-Phenyl-C61-butyric Acid Dimethylamino Ester as a Cathode Buffer Layer for High-Performance Polymer Solar Cells. *Adv. Energy Mater.* **2013**, *23*, 1569–1574.
31. Duan, C. H.; Cai, W. Z.; Hsu, B. B. Y.; Zhong, C. M.; Zhang, K.; Liu, C. C.; Hu, Z. C.; Huang, F.; Bazan, G. C.; Heeger, A. J.; *et al.* Toward Green Solvent Processable Photovoltaic Materials for Polymer Solar Cells: the Role of Highly Polar Pendant Groups in Charge Carrier Transport and Photovoltaic Behavior. *Energy Environ. Sci.* **2013**, *6*, 3022–3034.
32. Zhang, Z. G.; Li, H.; Qi, B. Y.; Chi, D.; Jin, Z. W.; Qi, Z.; Hou, J. H.; Li, Y. F.; Wang, J. Z. Amine Group Functionalized Fullerene Derivatives as Cathode Buffer Layers for High Performance Polymer Solar Cells. *J. Mater. Chem. A* **2013**, *1*, 9624–9629.
33. Duan, C. H.; Zhong, C. M.; Liu, C. C.; Huang, F.; Cao, Y. Highly Efficient Inverted Polymer Solar Cells Based on an Alcohol Soluble Fullerene Derivative Interfacial Modification Material. *Chem. Mater.* **2012**, *24*, 1682–1689.
34. Zhou, Y.; Fuentes-Hernandez, C.; Shim, J.; Meyer, J.; Giordano, A. J.; Li, H.; Winget, P.; Papadopoulos, T.; Cheun, H.; Kim, J.; *et al.* A Universal Method to Produce Low−Work Function Electrodes for Organic Electronics. *Science* **2012**, *336*, 327–332.
35. Wei, Q. S.; Nishizawa, T.; Tajima, K.; Hashimoto, K. Self-Organized Buffer Layers in Organic Solar Cells. *Adv. Mater.* **2008**, *20*, 2211–2216.
36. Jung, J. W.; Jo, J. W.; Jo, W. H. Enhanced Performance and Air Stability of Polymer Solar Cells by Formation of a Self-Assembled Buffer Layer from Fullerene-End-Capped Poly(ethylene glycol). *Adv. Mater.* **2011**, *23*, 1782–1787.
37. Yamakawa, S.; Tajima, K.; Hashimoto, K. Buffer Layer Formation in Organic Photovoltaic Cells by Self-Organization of Poly(dimethylsiloxane)s. *Org. Electron.* **2009**, *10*, 511–514.
38. Chen, F. C.; Chien, S. C. Nanoscale Functional Interlayers Formed through Spontaneous Vertical Phase Separation in Polymer Photovoltaic Devices. *J. Mater. Chem.* **2009**, *19*, 6865–6869.
39. Wang, H. T.; Zhang, W. F.; Xu, C. H.; Bi, X. H.; Chen, B. X.; Yang, S. F. Efficiency Enhancement of Polymer Solar Cells by Applying Poly(vinylpyrrolidone) as a Cathode Buffer Layer *via* Spin Coating or Self-Assembly. *ACS Appl. Mater. Interfaces* **2013**, *5*, 26–34.
40. Zhang, W. F.; Wang, H. T.; Chen, B. X.; Bi, X. H.; Venkatesan, S.; Qiao, Q. Q.; Yang, S. F. Oleamide as a Self-Assembled Cathode Buffer Layer for Polymer Solar Cells: the Role of the Terminal Group on the Function of the Surfactant. *J. Mater. Chem.* **2012**, *22*, 24067–24074.
41. Xu, Z.; Chen, L. M.; Yang, G. W.; Huang, C. H.; Hou, J. H.; Wu, Y.; Li, G.; Hsu, C. S.; Yang, Y. Vertical Phase Separation in Poly(3-hexylthiophene): Fullerene Derivative Blends and its Advantage for Inverted Structure Solar Cells. *Adv. Funct. Mater.* **2009**, *19*, 1227–1234.
42. Chen, L. M.; Hong, Z. R.; Li, G.; Yang, Y. Recent Progress in Polymer Solar Cells: Manipulation of Polymer:Fullerene Morphology and the Formation of Efficient Inverted Polymer Solar Cells. *Adv. Mater.* **2009**, *21*, 1434–1449.
43. Guerrero, A.; Dörling, B.; Ripolles-Sanchis, T.; Aghamohammadi, M.; Barrena, E.; Campoy-Quiles, M.; Garcia-Belmonte, G. Interplay between Fullerene Surface Coverage and Contact Selectivity of Cathode Interfaces in Organic Solar Cells. *ACS Nano* **2013**, *7*, 4637–4646.
44. Liao, S. H.; Jhuo, H. J.; Cheng, Y. S.; Chen, S. A. Fullerene Derivative-Doped Zinc Oxide Nanofilm as the Cathode of Inverted Polymer Solar Cells with Low-Bandgap Polymer (PTB7-Th) for High Performance. *Adv. Mater.* **2013**, *25*, 4766–4771.
45. You, J. B.; Dou, L. T.; Yoshimura, K.; Kato, T.; Ohya, K.; Moriarty, T.; Emery, K.; Chen, C. C.; Gao, J.; Li, G.; Yang, Y. A Polymer Tandem Solar Cell with 10.6% Power Conversion Efficiency. *Nat. Commun.* **2013**, *4*, 1446.

46. Hua, Z.; Zheng, Y.; Liu, N. L.; Ai, N.; Wang, Q.; Wu, S.; Zhou, J. H.; Hu, D. G.; Yu, S. F.; Han, S. H.; *et al.* All-Solution Processed Polymer Light-Emitting Diode Displays. *Nat. Commun.* **2013**, *4*, 1971.
47. Krebs, F. C. Polymer Solar Cell Modules Prepared Using Roll-to-Roll Methods: Knife-over-Edge Coating, Slot-Die Coating and Screen Printing. *Sol. Energy Mater. Sol. Cells* **2009**, *93*, 465–475.
48. Van Oss, C. J.; Ju, L.; Chaudhury, M. K.; Good, R. J. Estimation of the Polar Parameters of the Surface Tension of Liquids by Contact Angle Measurements on Gels. *J. Colloid Interface Sci.* **1989**, *128*, 313–319.
49. Van Oss, C. J.; Chaudhury, M. K.; Good, R. J. Interfacial Lifshitz-van der Waals and Polar Interactions in Macroscopic Systems. *Chem. Rev.* **1988**, *88*, 927–941.
50. Ma, K. X.; Chung, T. S.; Good, R. J. Surface Energy of Thermotropic Liquid Crystalline Polyesters and Polyesteramide. *J. Polym. Sci., Part B: Polym. Phys.* **1998**, *36*, 2327–2337.
51. Clark, M. D.; Jespersen, M. L.; Patel, R. J.; Leever, B. J. Predicting Vertical Phase Segregation in Polymer-Fullerene Bulk Heterojunction Solar Cells by Free Energy Analysis. *ACS Appl. Mater. Interfaces* **2013**, *5*, 4799–4807.